Structural, spectral and potentiometric characterization, and antimicrobial activity studies of [Zn(phen)$_2$(cnge)(H$_2$O)](NO$_3$)$_2$· H$_2$O

Leonor L. López Tévez [a] , María S. Islas [b] , Juan J. Martínez
Medina [a] , Maximiliano Diez [a] , Oscar E. Piro [c] , Eduardo E.
Castellano [d] , Evelina G. Ferrer [b] & Patricia A.M. Williams [b]

[a] Departamento de Química , UNCAUS , Cte. Fernández 755
(3700), Chaco , Argentina

[b] Centro de Química Inorgánica (CEQUINOR), FCE , UNLP, 47 y 115
(1900) La Plata, Argentina

[c] Departamento de Física, Facultad de Ciencias Exactas ,
Universidad Nacional de La Plata and Instituto IFLP (CONICET,
CCT-La Plata) , C.C. 67, 1900 La Plata, Argentina

[d] Instituto de Física de São Carlos , Universidade de São Paulo ,
C.P. 369, 13560 São Carlos, SP, Brazil
Accepted author version posted online: 11 May 2012.Published
online: 29 May 2012.

PLEASE SCROLL DOWN FOR ARTICLE

Structural, spectral and potentiometric characterization, and antimicrobial activity studies of [Zn(phen)₂(cnge)(H₂O)](NO₃)₂ · H₂O

LEONOR L. LÓPEZ TÉVEZ†, MARÍA S. ISLAS‡,
JUAN J. MARTÍNEZ MEDINA†, MAXIMILIANO DIEZ†, OSCAR E. PIROS§,
EDUARDO E. CASTELLANO¶, EVELINA G. FERRER‡ and
PATRICIA A.M. WILLIAMS*‡

†Departamento de Química, UNCAUS, Cte. Fernández 755 (3700), Chaco, Argentina
‡Centro de Química Inorgánica (CEQUINOR), FCE, UNLP,
47 y 115 (1900) La Plata, Argentina
§Departamento de Física, Facultad de Ciencias Exactas, Universidad Nacional
de La Plata and Instituto IFLP (CONICET, CCT-La Plata),
C.C. 67, 1900 La Plata, Argentina
¶Instituto de Física de São Carlos, Universidade de São Paulo,
C.P. 369, 13560 São Carlos, SP, Brazil

An octahedral Zn complex with *o*-phenanthroline (*o*-phen) and cyanoguanidine (cnge) has been synthesized and characterized. The crystal structural data show the formation of a ZnN₅O core where the metal coordinates to two mutually perpendicular *o*-phenanthrolines as bidentate ligands [Zn–N bond lengths in the 2.124(2)–2.193(2) Å range], the cyanide nitrogen of a cnge [d(Zn–N) = 2.092(2) Å, ∠(Zn–N–C) = 161.1(2)°], and a water molecule [d(Zn–Ow) = 2.112(2) Å]. Spectral data (FT-IR, Raman, and fluorescence) and speciation studies are in agreement with the structure found in the solid state and the one proposed to exist in the solution. To evaluate the changes in the microbiological activity of Zn, antibacterial studies were carried out by observing the changes in minimum inhibitory concentration of the complex, the ligands, and the metal against five different bacterial strains. The antibacterial activity of Zn improved upon complexation in three of the tested strains.

Keywords: *o*-Phenanthroline; Cyanoguanidine; Zinc complex; Crystal structure; Antibacterial properties

1. Introduction

Zinc is an essential metal, widely distributed in cells, and is the most abundant intracellular trace element. Catalytic, structural, and regulatory are the main biological roles played by the biometal [1]. In metalloproteins such as superoxide dismutase cytosolic CuZn, zinc plays a structural role while the copper functions as the catalytic

---

*Corresponding author. Email: williams@quimica.unlp.edu.ar

site. The structural stabilization role played by zinc in the folding of metalloproteins named zinc fingers, located in many membrane receptors and transcription factors, has been determined. The biometal is also important in the synthesis of proteins, nucleic acids, and cell division. Zn plays an important function in the immune system and Zn depletion is followed by a decrease in the cell-mediated immune response. Considering the participation in antioxidant processes, Zn is able to protect and stabilize cell membranes as well as vitamin E [2].

Complexation is associated with zinc in biological systems; the nanomolar concentration of Zn in body fluids and tissues is due to the presence of functional groups capable of forming coordinate covalent bonds. To supply the free metal ion required for enzymatic synthesis facilitating Zn-dependent biochemical processes, the most advantageous biological release is the use of low molecular weight chelates or complexes of Zn [3].

Model systems were developed to establish the mode of action of natural systems containing transition metals. To simulate nitrogen environments around Zn(II), we propose the use of cyanoguanidine (cnge) and *o*-phenanthroline (*o*-phen). cnge is the dimeric form of cyanamide, the latter being recently recognized as a substrate for nitrogenase containing cyano and guanidine that can coordinate with various metals [4–6]. Similar studies concerning the preparation, characterization, and *in vitro* biological activity determinations using copper(II) and cadmium(II) coordination compounds were reported previously [7, 8].

The $[Zn(phen)_2(cnge)(H_2O)](NO_3)_2 \cdot H_2O$ complex was synthesized at high pH and the crystal structure was determined by X-ray diffraction methods. The complex was characterized both in the solid state and in the solution by FT-IR, Raman, and fluorescence spectroscopies, respectively. The ligands, the metal, and the metal complex were tested *in vitro* against five strains for their antimicrobial effects to determine the possible improvement of these effects upon complexation. The species distribution was studied by potentiometric techniques to find out which is the majority species at equilibrium under physiological conditions that will directly interact with bacteria.

2. Experimental

2.1. *Materials and measurements*

All chemicals were of analytical grade [$ZnCl_2$ (Merck, Merck Química Argentina S.A.I.C.), $Zn(NO_3)_2 \cdot 6H_2O$ (Merck, Merck Química Argentina S.A.I.C.), cnge (Fluka, Sigma Aldrich de Argentina SA) and *o*-phenanthroline (Sigma, Sigma Aldrich de Argentina SA)] and used as purchased. Elemental analyses for carbon, nitrogen, and hydrogen were performed using a Carlo Erba EA 1108 analyzer. FT-IR spectra of powdered samples were recorded with a Bruker IFS 66 FT-IR-spectrophotometer from 4000 to 400 cm^{-1} as pressed KBr pellets. Raman spectra were collected on a Bruker IFS 113 FT-IR spectrophotometer provided with the NIR Raman attachment equipped with a Nd:YAG laser at 1064 nm. Thermogravimetric (TG) measurements were performed on a Shimadzu system (model TG-50) working in an oxygen flow (50 mL min^{-1}) at a heating rate of 10°C min^{-1}. Sample quantities ranged from 10 to

20 mg. Excitation and emission spectra were obtained on a Perkin-Elmer LS-50B luminescence spectrometer (Beaconsfield, England) equipped with a pulsed xenon lamp as the excitation source (half peak height $< 10\,\mu s$, 60 Hz), an R928 photomultiplier tube and a computer with FL Winlab software. Quartz cells of 1 cm path length were used and both excitation and emission slits were 10 nm wide. Scan speed was $500\,nm\,min^{-1}$. To determine the stability of the complex under the conditions of the biological studies, the solid complex and its components were dissolved in DMSO : water (50 : 50 v/v). Both electronic and fluorescence spectra were recorded as a function of time. Quartz cells of 1 cm path length were used. The excitation and emission slits used in the fluorometric determinations were 15 nm wide and the scan speed was $500\,nm\,min^{-1}$.

2.2. *Synthesis of the complex*

[Zn(phen)$_2$(cnge)(H$_2$O)](NO$_3$)$_2$ · H$_2$O: To a solution of cnge (1 mmol) in water (5 mL), an aqueous solution of Zn(NO$_3$)$_2$ (1 mmol, 5 mL) was added with continuous stirring. Several minutes later, an ethanolic solution of *o*-phenanthroline (2 mmol, 5 mL) was added. The pH of the colorless solution was raised to 10 with NaOH (1 mol L^{-1}) and the solution was stirred for about 15 min. The white precipitate was filtered and discarded. After 2 weeks of slow evaporation at room temperature, the mother liquor showed the formation of colorless single-crystals suitable for X-ray diffraction work. Anal. Calcd for C$_{26}$H$_{24}$N$_{10}$O$_8$Zn (%): C, 46.6; H, 3.6; N, 20.9. Found (%): C, 45.8; H, 3.7; N, 21.2. To determine the number of water molecules in the complex, the thermal decomposition was measured from 20°C to 200°C. The decomposition process recorded in the TG curve involves the release of two water molecules in two different steps. The first at 78°C can be assigned to a crystallization water (mass loss Calcd 2.69%, Found 2.63%). The second step at 110°C involves the loss of a bound water (coordinated water, mass loss Calcd 2.69%, Found 2.69%). Two endothermic peaks appearing within the above thermal range in the DTA study support the assignments.

2.3. *X-ray diffraction data*

Single-crystal X-ray diffraction measurements for [Zn(phen)$_2$(cnge)(H$_2$O)](NO$_3$)$_2$ · H$_2$O were carried out at low temperature on an Enraf-Nonius Kappa-CCD diffractometer with graphite-monochromated Mo-Kα ($\lambda = 0.71073$ Å) radiation. Diffraction data were gathered (φ and ω scans with κ-offsets) with COLLECT [9]. Integration and scaling of the reflections were performed with HKL DENZO-SCALEPACK [10] suite of programs. The unit cell parameters were obtained by least-squares refinement based on angular settings for all collected reflections using HKL SCALEPACK [9]. The structure was solved by direct methods with SHELXS-97 [11] and the corresponding molecular model developed by alternated cycles of Fourier methods and full-matrix least-squares refinement on F^2 with SHELXL-97 [12]. A difference Fourier map phased on the non-H atoms of [Zn(phen)$_2$(cnge)(H$_2$O)](NO$_3$) molecular fragment showed that the other nitrate and the crystallization water are severely disordered in the lattice. This disorder could not be modeled adequately in terms of the expected molecules. Therefore, we proceeded with the refinement of the ordered [Zn(phen)$_2$(cnge)(H$_2$O)](NO$_3$) partial

Table 1. Crystal data and structure refinement for the ordered [Zn(phen)$_2$(cnge)(H$_2$O)](NO$_3$) partial structure in the [Zn(phen)$_2$(cnge)(H$_2$O)](NO$_3$)$_2$.H$_2$O solid.

Empirical formula	C$_{26}$H$_{22}$N$_9$O$_4$Zn
Formula weight	589.90
Temperature (K)	100(2)
Wavelength (Å)	0.71073
Crystal system	Monoclinic
Space group	$P2_1/c$
Unit cell dimensions (Å, °)	
a	13.0273(3)
b	18.4151(4)
c	13.6855(3)
β	10.71(1)
Volume (Å^3), Z	3070.99(12), 4
Calculated density (Mg m^{-3})	1.449
Absorption coefficient (mm^{-1})	0.86
$F(000)$	1212
Crystal size (mm^3)	0.20 × 0.12 × 0.12
θ range for data collection (°)	2.72–26.00
Limiting indices	$-16 \leq h \leq 16$;
	$-22 \leq k \leq 22$;
	$-16 \leq l \leq 16$
Reflections collected	25,823
Independent reflections	6016 [R(int) = 0.0411]
Observed reflections [$I > 2\sigma(I)$]	5157
Completeness to $\theta = 26.00$ (%)	99.7
Max. and min. transmission	0.9055 and 0.8494
Refinement method	Full-matrix least-squares on F^2
Data/restraints/parameters	6016/3/369
Goodness-of-fit on F^2	1.068
Final R indices[a] [$I > 2\sigma(I)$]	$R_1 = 0.0419$, $wR_2 = 0.1235$
R indices (all data)	$R_1 = 0.0479$, $wR_2 = 0.1273$
Largest difference peak and hole (e Å^{-3})	0.356 and -0.682

[a] $R_1 = \Sigma||F_o|-|F_c||/\Sigma|F_o|$, $wR_2 = [\Sigma w(|F_o|^2-|F_c|^2)^2/\Sigma w(|F_o|^2)^2]^{1/2}$.

structure resorting to a procedure described [13] and implemented in the program SQUEEZE included in the PLATON [14] suite of programs. The hydrogen atoms were located in a Fourier difference map. However, all but water hydrogen atoms were positioned stereochemically and refined with the riding model. The water hydrogen atoms were refined at their found positions restraining their Ow–H and H$\cdots$H distances to target values of 0.86(1) and 1.36(1) Å. Crystal data, data collection procedure, structure determination methods, and refinement results are summarized in table 1.

2.4. *Potentiometric measurements*

The stability constants of complexes and the protonation constants of the ligands were determined at 298 K, 0.150 mol L^{-1} ionic strength (NaCl) and under nitrogen, as previously described [7, 8]. A Schott Gerate TS165 pH meter was used for EMF measurements and the added volumes were measured using a Techware (Sigma) Digitrate (25 mL). All solutions were prepared prior to their use with freshly deionized and carbonate-free tridistilled water which was cooled under a constant flow of nitrogen. Diluted solutions of HCl (Merck p.a.) were standardized against TRISMA-base (hydroxymethyl aminomethane). Diluted NaOH solutions were

prepared from a saturated NaOH solution and standardized against the HCl. The glass electrode was calibrated separately in a solution with known [H$^+$] before and after each titration. Different metal-to-ligand ratios were selected in order to prevent precipitation. Zinc solutions were prepared by dissolving ZnCl$_2$ (Merck) and the data were collected from the lowest pH that could be reached in the experiment up to pH = 11.

2.5. *Antibacterial assays*

The following strains of bacteria derived from the American Type Culture Collections (ATCC) were used for screening: *Escherichia coli* (ATCC 35218), *Pseudomonas aeruginosa* (ATCC 27853), *Staphylococcus aureus* (ATCC 25923), *Staphylococcus epidermidis* (ATCC 1263), and *Enterococcus faecalis* (ATCC 29212). The cultivation/ assay medium for all strains was Mueller Hinton Broth or Agar (MHB, MHA) [15].

The inoculum was prepared by picking three to five colonies of the test organism and transferring into 5 mL of Mueller Hinton broth. The broth cultures were incubated overnight at 37°C and used to prepare an organism suspension in MHB. The suspensions were adjusted to 0.5 McFarland standard turbidity ($\sim$10^8 colony forming units (CFU) per milliliter). Cultures were diluted in 0.85% saline solution to a density of 1×10^7 CFU mL^{-1} [16–18].

The minimum inhibitory concentration (MIC) was determined by the agar-dilution method. The complex was dissolved in 50% aqueous DMSO to a final concentration of 66.9 mgmL^{-1}. Serial two-fold water dilutions were prepared from the stock solution of the antimicrobial agents to give concentrations ranging from 0.2 to 60 mg mL^{-1}. Aqueous solutions (120 mg mL^{-1}) of the metal salt and phen were prepared and twofold serial dilutions from 7.3×10^{-3} to 120 mg mL^{-1} were performed. Sterile solutions were used. Then, 0.5 mL of each dilution of antimicrobial solution was added to 4.5 mL of melted MHA and poured into a square (45 × 15 mm) plate. An agar plate without antibacterial agent was established as a sterility and organism growth control. The plates were prepared and used on the same day. After cooling and drying, the plates were inoculated with each bacterial cell suspension. The inoculum of 2 µL of the germ suspensions containing 1×10^7 CFU mL^{-1} were streaked onto the plates and incubated for 24 h at 37°C. Each MIC experiment was repeated thrice. MICs were interpreted after 24 h incubation at 37°C in ambient air. Inhibition of bacterial growth in the plates containing tested solutions was judged by comparing with growth in control plates. The MIC was defined as the lowest dilution of the complex that inhibited visible growth of the test organism. A single colony or a faint haze caused by the inoculum was considered to be no growth [16–22].

3. Results and discussion

3.1. *Structural results*

Figure 1 is an ORTEP [13] drawing of [Zn(phen)$_2$(cnge)(H$_2$O)] complex. Intramolecular bond distances and angles around zinc(II) are given in table 2. Zinc(II) is in a distorted octahedral environment, coordinated to two nearly planar [*rms* deviation of atoms from the best least-squares plane less than 0.055 Å] bidentate and mutually perpendicular
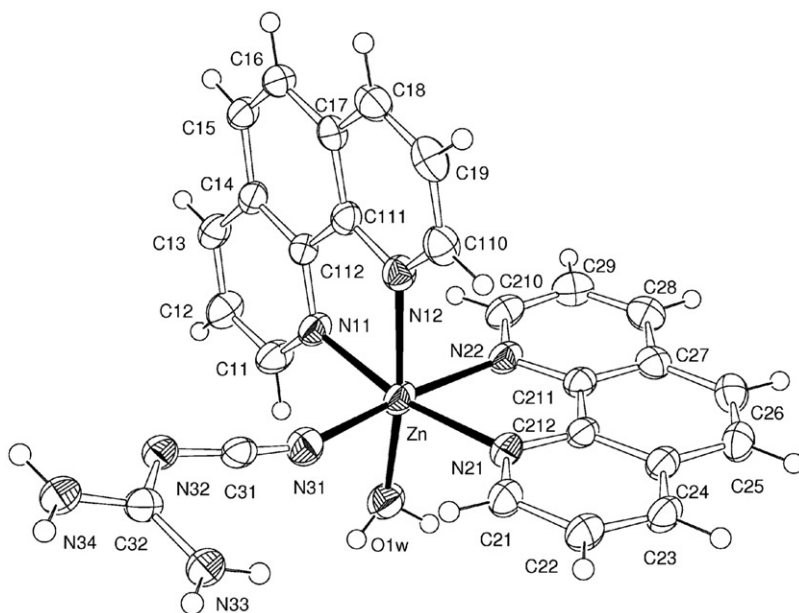
Figure 1. View of the Zn(II) complex in the [Zn(phen)$_2$(cnge)(H$_2$O)](NO$_3$)$_2$ · H$_2$O solid showing the labels of the non-H atoms and their displacement ellipsoids at the 50% probability level. Zinc–ligand bonds are indicated by full lines.

Table 2. Bond lengths (Å) and angles (°) around Zn(II) in [Zn(phen)$_2$(cnge)(H$_2$O)].

N(11)–Zn	2.124(2)
N(12)–Zn	2.193(2)
N(21)–Zn	2.136(2)
N(22)–Zn	2.189(2)
N(31)–Zn	2.092(2)
O(1 W)–Zn	2.112(2)
N(31)–Zn–O(1 W)	91.00(9)
N(31)–Zn–N(11)	94.01(8)
O(1 W)–Zn–N(11)	91.76(8)
N(31)–Zn–N(21)	94.84(8)
O(1 W)–Zn–N(21)	95.46(8)
N(11)–Zn–N(21)	168.47(8)
N(31)–Zn–N(22)	171.95(8)
O(1 W)–Zn–N(22)	90.55(8)
N(11)–Zn–N(22)	93.84(8)
N(21)–Zn–N(22)	77.15(8)
N(31)–Zn–N(12)	91.08(8)
O(1 W)–Zn–N(12)	168.98(7)
N(11)–Zn–N(12)	77.29(8)
N(21)–Zn–N(12)	95.15(8)
N(22)–Zn–N(12)	88.89(8)

phen [dihedral angle of 88.82(3)°] [Zn–N bond lengths ranging from 2.124(2) Å to 2.193(2) Å]. These distances are in agreement with other zinc(II) complexes with phen [23]. The remaining two *cis*-positions are occupied by cyanide nitrogen of cnge [d(Zn–

Table 3. Vibrational frequencies of $[Zn(cnge)(phen)_2(H_2O)](NO_3)_2 \cdot H_2O$, cnge and *o*-phen (cm^{-1}).

$[Zn(cnge)(phen)_2(H_2O)](NO_3)_2 \cdot H_2O$	cnge	*o*-phen	Assignments
2189 s	2208 m		$\nu(C\equiv N)$ cnge
2186 mw	2204 m		
2148 s	2162 s		$\nu(C\equiv N)$ cnge
2153, 2147 mw	2158 vs		
1647 sh, 1636 s, 1629 sh	1637 ms	1645 m, 1620 w	$\nu(C=N)$
1627 m	1647 w, 1635 w	1617 w	
1606 m,1586 m		1585 m	*o*-phen
		1601 w, 1590 w	
1569 s, 1552 s	1570 s	1558 m	$\nu(C=N)$
	1543 w	1564 vw	
1516 s, 1491 sh	1505 m	1501 s	
1518 m	1524 w	1503 w	
1423 s		1418 s	*o*-phen
1455 s, 1423 vs		1447 m, 1405 vs	
1380 vs			$\nu_3(E')$ NO_3^-
1381 vw			
1353 sh		1341 m	*o*-phen
1344 w, 1319 sh		1345 w	
1308 sh		1297 w	*o*-phen
1308 m		1295 m	
1250 m	1252 m	1273 w	
1255 w			
1223 m		1215 w	*o*-phen
1226 vw, 1207 vw			
1196 w		1183 w	*o*-phen
1141 m, 1098 m	1086 m	1090 m	
1148 w, 1106 w	1098 w	1090 w	
1055 m			$\nu_1(A'_1)$ NO_3^-
1042 m		1034 w	*o*-phen
1045 sh		1036 m	
997 m		990 w	
962 m		961 w	*o*-phen
968 vw			
920 m	928 m		$\nu_s(C\equiv N)$ cnge
921 w, 900 w	934 s		
856 sh, 847 s		852 vs	*o*-phen
867 w			
773 m, 754 sh		776 w	*o*-phen
724 s	723 w	738 vs	*o*-phen
732 m		711 m	
664 sh	671 m	693 m	
664 vw	667 m		
424 w	465 m	448 m	

s, strong; m, medium; mw, medium-weak; w, weak; vw, very weak; sh, shoulder.

N) $= 2.092(2)$ Å] that enters coordination slightly bent $[\angle(Zn\text{–}N\text{–}C) = 161.1(2)°]$ and a water molecule $[d(Zn\text{–}Ow) = 2.112(2)$ Å].

3.2. *Vibrational spectroscopic properties*

FT-IR and Raman spectra were measured to $400\,cm^{-1}$. Vibration bands and corresponding assignments for cnge, phen, and $[Zn(cnge)(phen)_2(H_2O)](NO_3)_2 \cdot H_2O$ are given in table 3. The tentative assignments were based on the reported ones [24–26] and our previous work [7, 8]. The characteristic phen strong bands at 850 and $721\,cm^{-1}$ are observed in the complex with small shifts and different intensities due to

coordination. The asymmetric stretching doublet (ν_{as}(NCN)) for free cnge also shifts on coordination. These modes were red or blue shifted in copper(II) cnge *o*-phenanthroline complexes, depending on the metal-N(cnge) distance [7]. In a previous paper ternary complexes of copper cnge with different anions were reported. Shorter Cu–N(cnge) distances and M–N–C angles close to 180° were indicative of stronger Cu–cnge interactions and the ν(C≡N) doublet exhibited the most pronounced shift to higher energy. On the contrary, weaker Cu–N(cnge) bonds and lower angles produced red shifts [25]. In the present complex a shift of this vibrational mode to lower wavenumbers (from 2212–2162 cm^{-1} to 2189–2148 cm^{-1}) is observed, in concordance with a longer Zn–N distance (2.092 Å), a lower Zn–N–C angle (161°) and a subsequent weakness of the coordination. The totally symmetric valence vibrations of C≡N bonds fall in the 930 cm^{-1} region (a strong band at 934 cm^{-1} in the Raman spectrum of cnge) [27]. As expected, the Raman intensity of this mode weakens upon coordination (table 3).

The vibrational modes of nitrate in the FT-IR and Raman spectra allow determination of the possible coordination. The band ν_3(E′) at 1380 cm^{-1} is indicative of the presence of unbonded nitrate (free D$_{3h}$ symmetry). The Raman active symmetric stretch ν_1(A$_1'$) located at 1055 cm^{-1} confirms that the nitrate is present as counter-ion in the Zn complex [24].

3.3. *Solution equilibria*

Protonation constants of the ligands (LH = cngeH and AH$^+$ = *o*-phenH$^+$) were redetermined in the pH-potentiometric measurements of the Zn(II)-ligand systems. The log K values are in agreement with those measured by us under identical conditions [7, 8]. The experimental log β_{0101} value of 5.0 for *o*-phenH$^+$ was recalculated and found in agreement with the reported value [28, 29].

The stability constants of the ternary complexes were refined separately using the titration data of these systems (using the Best computer program and Superquad) [30]. Then, those values were fixed and consequently only quaternary species were refined in the final model. Sets of titrations with varying total concentrations and concentration ratios of the components were carried out to establish the equilibria of the quaternary system Zn^{2+}/*o*-phen/cnge/H$^+$.

The formation constants denoted by β_{pqrs} correspond to the general notation:

$$\text{p Zn}^{2+} + \text{q } o-\text{phen} + \text{r cnge} + \text{s H}^+ \otimes \left(\text{Zn}^{2+}\right)_p (\text{phen})_q (\text{cnge})_r \left(\text{H}^+\right)_s$$

A value of pK_w = 13.76 (equivalent to log β_{000-1} = −13.76) was assumed for the experimental conditions (T = 298 K, I = 150 mmol L^{-1}).

To fit the potentiometric data with Superquad, different species were considered and the best model was refined. The stability constants (log β) of the ternary system (Zn^{2+}/cnge/H$^+$) are reported in table 4. These values were used to compute the species distribution curve that is shown in figure 2.

It can be seen that in the ternary Zn^{2+}/cnge/H$^+$ system a competition between free Zn^{2+} and [ZnL$_2$H$_2$]$^{+2}$ exist from pH 3.5 to pH 6.5 (log β_{122} = 32.31). Formation of hydroxo complexes were observed at higher pH values. In addition, the stability constants calculated for the Zn^{2+}/*o*-phen/H$^+$ system are in good accordance with the previous results [29, 31].

Table 4. Composition, notation, and formation constants (β) for the Zn^{2+}/cnge (L)/H^+ system (0.150 mol L^{-1} NaCl, 298 K).

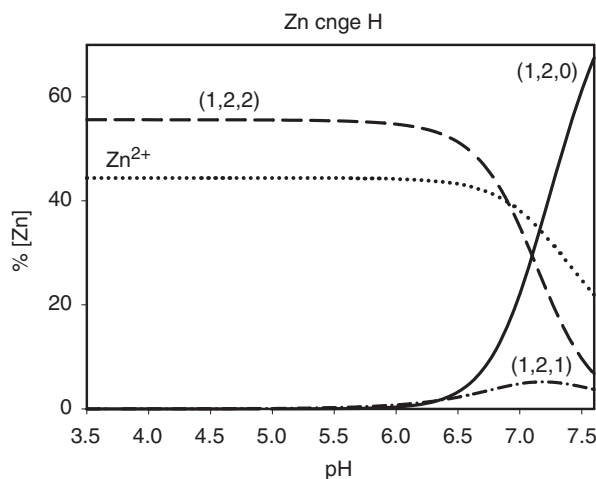| Species (pqr)	Formula	log β
011	LH	11.57
10−1	$[ZnH_{-1}]^{1+}$	10.20
10−2	$[ZnH_{-2}]$	19.40
10−3	$[ZnH_{-3}]^{-}$	27.70
10−4	$[ZnH_{-4}]^{2-}$	37.20
11−3	$[ZnLH_{-3}]^{-}$	−16.58
122	$[ZnL_2H_2]^{+2}$	32.31
121	$[ZnL_2H]^{+1}$	23.91
120	$[ZnL_2]$	17.30

Figure 2. Species distribution patterns of the Zn(II) complexes in the binary system Zn^{2+}/cnge (L)/H^+ as a function of pH. Total concentrations: Zn^{2+}, 0.1 mmol L^{-1} and cnge, 0.2 mmol L^{-1}, 25°C, $I = 0.150$ mol L^{-1} NaCl.

Table 5. Composition, notation, and formation constants (β) for the Zn^{2+}/o-phen(A)/cnge (L)/H+ system (0.150 mol L^{-1} NaCl, 298 K).

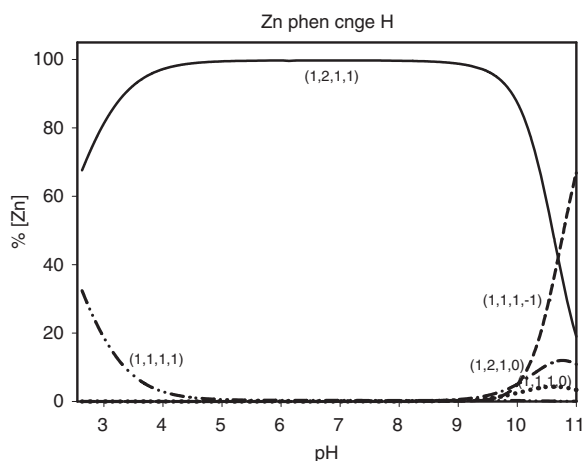| Species (pqrs)	Formula	log β
0011	LH	11.57
0101	AH	4.96
1100	$[ZnA]^{2+}$	6.40
1200	$[ZnA_2]^{2+}$	12.20
1300	$[ZnA_3]^{2+}$	17.00
1020	$[ZnL_2]$	17.30
1021	$[ZnL_2H]^{+}$	23.91
1022	$[ZnL_2H_2]^{+2}$	32.31
1211	$[ZnA_2LH]^{+2}$	37.90
1210	$[ZnA_2L]^{+}$	26.66
1111	$[ZnALH]^{+2}$	32.07
1110	$[ZnAL]^{+}$	23.08
111-1	$[ZnALH_{-1}]$	13.38

Figure 3. Species distribution patterns of the Zn(II) complexes in the ternary system Zn^{2+}/o-phen (A)/cnge (L)/H^+ as a function of pH. Total concentrations: Zn^{2+}, $0.5\,mmol\,L^{-1}$, phen, $1.5\,mmol\,L^{-1}$, and cnge, $1\,mmol\,L^{-1}$, 25°C, $I = 0.150\,mol\,L^{-1}$ NaCl.

The stoichiometry and stability constants of the quaternary complexes are collected in table 5. In acidic medium, complexes with one cnge and one or two phen are formed. The quaternary specie $[ZnA_2LH]^{2+}$ ($\log \beta_{1211} = 37.90$) becomes dominant at pH values between 4 and 9. When the pH is increased a proton loss (either from coordinated water molecule or cnge) is observed and the new specie ($[ZnAL–H]$, $\log \beta_{111-1} = 13.38$) prevails.

The percentages of the other quaternary species in the equilibrium are almost negligible under the selected experimental conditions. As can be seen from figure 3, the formation of a (1,2,1,1) species even at the concentration range used for antibacterial determinations (*ca* $1\,mmol\,L^{-1}$) allow us to postulate $[ZnA_2L]^+$ as the main species at neutral pH.

3.4. Fluorescent properties

Fluorescence spectra of the Zn complex were performed in water/ethanol (1/1) solutions for $1\,mmol\,L^{-1}$ of $ZnCl_2$, cnge, and the Zn complex and for $2\,mmol\,L^{-1}$ solutions of o-phenanthroline. Cnge did not show appreciable fluorescence. The spectrum of o-phenanthroline showed weak emissions at 358 and 377 nm ($\lambda_{ex} = 359$ nm) that correspond to a $\pi \to \pi^*$ transition [32]. The complex exhibited more intense blue fluorescent emission bands at 365, 377 (sh), and 405 (sh) nm upon photoexcitation at 334 nm (figures 4 and 5). Similar effects were also observed in the Cd, o-phen, cnge complex [8].

The enhancement of luminescence may be attributed to increased rigidity of the ligand (planar configuration) by metal coordination that reduces the loss of energy by radiationless decay. The band centered at 365 nm is tentatively assigned to the intraligand fluorescence of coordinated phen. These results are comparable with other Zn(II) mixed ligand complexes containing phen and other ligands, but care needs to be taken with the different reported experimental designs [33]. For instance, the
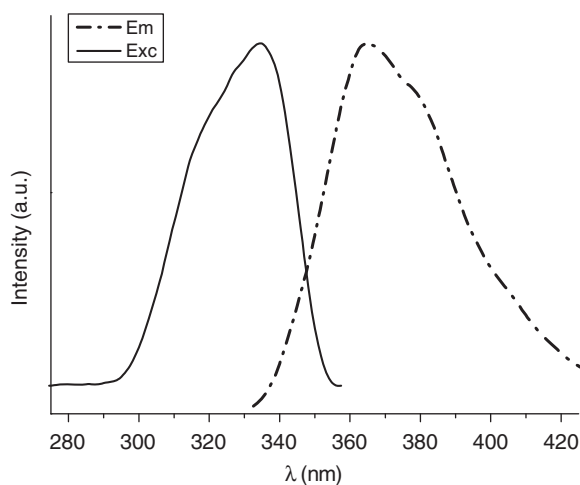
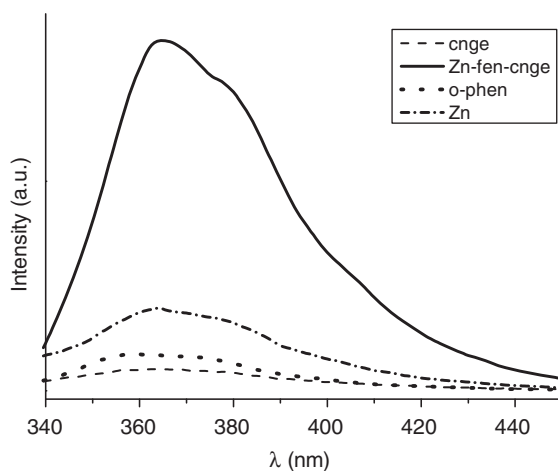Figure 4. Emission and excitation spectra of the Zn/cnge/phen complex in ethanol/water (1/1) solution.

Figure 5. Fluorescence emission spectra of ethanol/water (1/1) solutions of the Zn complex, $ZnCl_2$, cnge (1 mmol L^{-1}) and *o*-phenanthroline (2 mmol L^{-1}).

fluorescence spectrum of $[Zn(phen)(SO_4)(H_2O)_2]_n$ displayed a broad emission band in the blue light region (maximum emission peaks at 400, λ_{ex} 280 nm) [34]. This spectrum was red-shifted in comparison with the spectra of the aqueous solutions. These effects were ascribed to the exciplex emissions and revealed the strong interactions between molecules, generated by strong π–π stacking of the aromatic rings [35].

3.5. *Stability studies of the dissolved complex*

Ligand dissociation from the labile metal center can interfere with antimicrobial measurements, so we have undertaken stability studies of the dissolved compound. Stability determinations were followed spectrophotometrically using electronic and
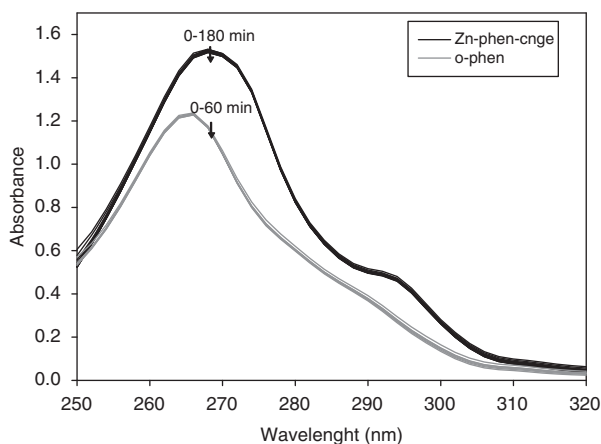
Figure 6. Time variation of the electronic spectra of *o*-phenanthroline $(5 \times 10^{-5}\,\mathrm{mol\,L^{-1}})$ and $[\mathrm{Zn(phen)_2(cnge)(H_2O)}](\mathrm{NO_3})_2 \cdot \mathrm{H_2O}$ $(2.5 \times 10^{-5}\,\mathrm{mol\,L^{-1}})$ in water : DMSO (50 : 50 v/v).
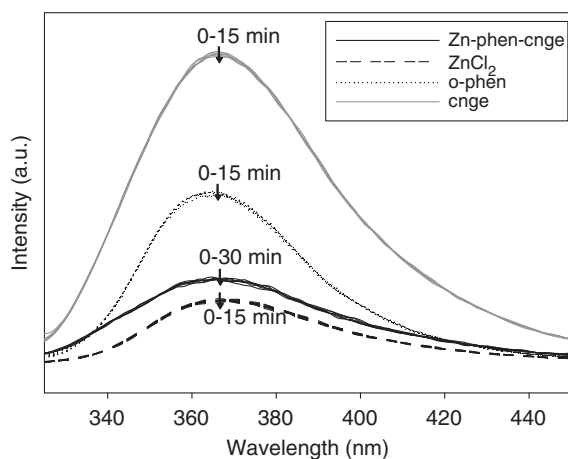

Figure 7. Change in fluorescence spectra with change in the time of a water : DMSO (50 : 50 v/v) solution of $\mathrm{ZnCl_2}$, $[\mathrm{Zn(phen)_2(cnge)(H_2O)}](\mathrm{NO_3})_2 \cdot \mathrm{H_2O}$ and cnge $(1 \times 10^{-3}\,\mathrm{mol\,L^{-1}})$ and *o*-phenanthroline $(2 \times 10^{-3}\,\mathrm{mol\,L^{-1}})$. Excitation wavelengths: 288 nm, 320 nm, 300 nm, and 316 nm, respectively.

fluorescence spectroscopies at least for 15 min, that is the time of manipulation of the solid dissolved in water : DMSO before its addition to the melted MHA and transfer to the square plate.

The electronic UV spectra of *o*-phenanthroline and the Zn ternary complex are displayed in figure 6. The ligand is stable for at least 1 h and the complex is stable during the 3 h of the spectroscopic determinations.

Fluorescence spectra of the complex and its components at different times are shown in figure 7. The dissolved complex remained stable for 15 min being the only species that can contribute to the antimicrobial assays.

Table 6. MICs of the Zn/cnge/*o*-phen complex, ZnCl$_2$, and *o*-phen for the reference strains, in $\mu g\,mL^{-1}$.

	E. coli	*S. aureus*	*S. epidermidis*	*E. faecalis*	*P. aeruginosa*
Zn/cnge/*o*-phen	47	94	94	3000	6000
ZnCl$_2$	188	188	188	1500	1500
o-phen	12	24	12	94	375

3.6. *Microbiological assays*

MIC of the metal, phen, and the complex are displayed in table 6. The tested strains are not susceptible to cnge.

Zinc is an essential metal for all living systems, including microbes and mammals, where the biological roles of zinc include metalloenzymes and membrane stabilization. Zinc ion concentrations of $10^{-5}-10^{-7}\,mol\,L^{-1}$ are required for optimal bacterial growth of most microorganisms *in vitro* [36], but it can became toxic at higher concentrations. Millimolar concentrations of ZnCl$_2$ are required to produce anti-bacterial activities for *E. coli*, *S. aureus*, *E. faecalis* [37], and *P. aeruginosa* [38]. These results are in agreement with those shown in table 6 (from *ca* 0.8 to 6 mmol L^{-1}).

o-Phenanthroline shows the lowest MIC values against the tested strains, as expected [39, 40]. Complexation with Zn produced a decrease of the antimicrobial activity of *o*-phenanthroline but an increase of the effect of the metal on *E. coli*, *S. aureus*, and *S. epidermidis*. In other tested strains *E. faecalis* and *P. aeruginosa*, the inhibition occurs at the highest concentrations for both the metal and the complex. However, the latter effects have no relevance from a clinical perspective (*in vitro* measurements of antibacterial activities with MIC values greater than 1000 $\mu g\,mL^{-1}$ are considered insignificant) [41, 42].

In a previous study [8] we investigated the antibacterial properties of [Cd(*o*-phen)$_2$(SO$_4$)(H$_2$O)](cnge) $\cdot$ 5H$_2$O. The measurements were performed using the disc diffusion method instead of MIC calculations. Nevertheless, a direct correlation between both techniques can be determined making comparisons with the values measured for *o*-phenanthroline. From potentiometric determinations, the same active species is expected to interact with bacteria at physiological conditions for the cadmium and the zinc complexes, ([M(phen)$_2$(cnge)]$^{2+}$). The toxic effect of cadmium is similar to that of *o*-phen (except in the case of *E. coli*) and it was improved upon complexation. The essential Zn(II) cation exerted a lower toxic effect than cadmium, but insignificant for *P. aeruginosa* and *E. faecalis* (greater than 1000 $\mu g\,mL^{-1}$). Its complexation with *o*-phenanthroline and cnge helps to improve its antimicrobial effect but not as large as the toxic effect of *o*-phenanthroline. The same behavior was observed for [Zn(bpy)$_2$(phen)]Cl$_2$ $\cdot$ 6H$_2$O [40].

4. Conclusion

The interaction of *o*-phen and cnge with Cu(II), Cd(II), and Zn(II) produced different coordination compounds with different environments and geometries (CuN$_5$, CuN$_3$O$_3$, CdN$_4$O$_2$, and ZnN$_5$O cores). The strength of the M–NC(cnge) bond, determined by

X-ray measurements, is essential for the blue or red shift of the antisymmetric-stretching CN band in the vibration spectra. Fluorescence measurements pointed to a strong rigidity of *o*-phen upon coordination. Speciation studies were performed to determine the active species at physiological pH. Majority of the species in the solution at 298 K, pH 7.4 and ionic strength 0.150 mol L^{-1} (NaCl), [ZnA$_2$LH]$^{2+}$, display the same coordination sphere as the solid nitrate salt. On forming coordination complexes with nitrogen containing bases at physiological conditions, the antibacterial activity of Zn against *E. coli*, *S. aureus*, and *S. epidermidis* was improved.

Supplementary material

Listings of fractional coordinates and equivalent isotropic displacement parameters for the non-H atoms of the [Zn(phen)$_2$(cnge)(H$_2$O)] complex are given in table S1, full intramolecular bond distances and angles in table S2, atomic anisotropic displacement parameters in table S3, and hydrogen atom positions in table S4. A CIF file containing details of the crystal structure reported in this article has been deposited with the Cambridge Crystallographic Data Center, reference number CCDC 854692.

Acknowledgments

References

[1] A.S. Prasad. *J. Am. Coll. Nutr.*, **2**, 113 (1996).
[2] A.S. Prasad. *Nutrition*, **11**, 93 (1995).
[3] P.M. May, P.W. Linder, D.R. Williams. *J. Chem. Soc., Dalton Trans.*, 588 (1977).
[4] A.S. Batsanov, P. Hubberstey, C.E. Russell, P.H. Walton. *J. Chem. Soc., Dalton Trans.*, 2667 (1997).
[5] J. Pickardt, B. Kühn. *Z. Kristallogr.*, **11**, 901 (1995).
[6] P.J. Bailey, S. Pace. *Coord. Chem. Rev.*, **214**, 91 (2001).
[7] E.G. Ferrer, L.L. López Tévez, N. Baeza, M.J. Correa, N. Okulik, L. Lezama, T. Rojo, E.E. Castellano, O.E. Piro, P.A.M. Williams. *J. Inorg. Biochem.*, **101**, 741 (2007).
[8] L.L. López Tévez, J.J. Martínez Medina, M.S. Islas, O.E. Piro, E.E. Castellano, L. Bruzzone, E.G. Ferrer, P.A.M. Williams. *J. Coord. Chem.*, **64**, 3560 (2011).
[9] Enraf-Nonius. *COLLECT*, B.V. Nonius, Delft, The Netherlands (1997-2000).
[10] Z. Otwinowski, W. Minor. In *Methods in Enzymology*, C.W. Carter Jr, R.M. Sweet (Eds), Vol. 276, pp. 307–326, Academic Press, New York (1997).
[11] (a) G.M. Sheldrick. *SHELXS-97, Program for Crystal Structure Resolution*, University of Göttingen, Göttingen, Germany (1997); (b) G.M. Sheldrick. *Acta Crystallogr. A*, **46**, 467 (1990).
[12] (a) G.M. Sheldrick. *SHELXL-97, Program for Crystal Structures Analysis*, University of Göttingen, Göttingen, Germany (1997); (b) G.M. Sheldrick. *Acta Crystallogr. A*, **64** 112 (2008).
[13] P. Van der Sluis, A.L. Spek. *Acta Crystallogr. A*, **46**, 194 (1999).

[14] A.L. Spek. *PLATON, A Multipurpose Crystallographic Tool*, Utrecht University, Utrecht, The Netherlands (1998).
[15] A. Klančnik, S. Piskernik, B. Jeršek, S. Smole Možina. *J. Microbiol. Meth.*, **81**, 121 (2010).
[16] O. Koru, M. Ozyurt. *Anaerobe*, **14**, 161 (2008).
[17] A. Berahou, A. Auhmani, N. Fdil, A. Benharref, M. Jana, C.A. Gadhi. *J. Ethnopharmacol.*, **112**, 426 (2007).
[18] C.E. Smith, B.E. Foleno, J.F. Barrett, M.B. Fresco. *Diagn. Microbiol. Infect. Dis.*, **27**, 85 (1997).
[19] G. Hall, A. Heimdahl, C.E. Nord. *Anaerobe*, **4**, 29 (1998).
[20] S. Weckesser, K. Engel, B. Simon-Haarhaus, A. Wittmer, K. Pelz, C.M. Schempp. *Phytomedicine*, **14**, 508 (2007).
[21] J.D. Gomez, N.M. Cudmani, M.A. Vattuone, M.I. Isla. *Life Sci.*, **75**, 191 (2004).
[22] M. Fang, J. Hua Chen, X. Li Xu, P. Hong Yang, H.F. Hildebrand. *Int. J. Antimicrob. Agents*, **27**, 513 (2006).
[23] E.-Ju. Gao, Q.-T. Liu. *J. Struct. Chem.*, **51**, 1132 (2010).
[24] K. Nakamoto. *Infrared and Raman Spectra of Inorganic and Coordination Compounds*, 4th Edn, Wiley, New York (1986).
[25] M.J. Begley, P. Hubberstey, P.H. Spittle, P.H. Walton. *Acta Cryst.*, **49**, 1047 (1993).
[26] M. Davies, W.J. Jones. *Trans. Faraday Soc.*, **54**, 1454 (1958).
[27] L.A. Sheludyakova, E.V. Sobolev, L.I. Kozhevina. *J. Appl. Spectrosc.*, **55**, 661 (1991).
[28] J.P. Scharff, M.R. Páris. *Bull. Soc. Chim. Fr.*, **5**, 1782 (1967).
[29] C.V. Banks, R.I. Bystroff. *J. Amer. Chem. Soc.*, **81**, 6153 (1959).
[30] A.E. Martell, R.J. Motekaitis. *Determination and Use of Stability Constants*, 2nd Edn, VCH, New York (1992).
[31] M.J. Fahsell, C.V. Banks. *J. Amer. Chem. Soc.*, **88**, 878 (1966).
[32] X. Shi, G. Zhu, Q. Fang, G. Wu, G. Tian, R. Wang, D. Zhang, M. Xue, S. Qiu. *Eur. J. Inorg. Chem.*, 185 (2004).
[33] R. Carballo, B. Covelo, C. Lodeiro, E.M. Vázquez-López. *Cryst. Eng. Comm.*, **7**, 294 (2005).
[34] X. Hu, J. Guo, C. Liu, H. Zen, Y. Wang, W. Du. *Inorg. Chim. Acta*, **362**, 3421 (2009).
[35] W. Guo, Z. Peng, D. Li, Y. Zhou. *Polyhedron*, **23**, 1701 (2004).
[36] B. Sugarman. *Rev. Infect. Dis.*, **5**, 137 (1983).
[37] S. Atmaca, K. Gül, R. Çiçek. *Tr. J. Med. Sci.*, **28**, 595 (1998).
[38] M. Fettouhi, M.I.M. Wazeer, A.A. Isab. *J. Coord. Chem.*, **60**, 369 (2007).
[39] S.B. Kalia, G. Kaushal, M. Kumar, S.S. Cameotra, A. Sharma, M.L. Verma, S.S. Kanwar. *Braz. J. Microbiol.*, **40**, 916 (2009).
[40] M.O. Agwara, P.T. Ndifon, N.B. Ndosiri, A.G. Paboudam, D.M. Yufanyi, A. Mohamadou. *Bull. Chem. Soc. Ehiop.*, **24**, 383 (2010).
[41] J.C.A. Tanaka, C.C. da Silva, A.J.B. de Oliveira, C.V. Nakamura, B.P. Dias Filho. *Brazilian J. Med. Biol. Res.*, **39**, 387 (2006).
[42] A.A. Aliero, A.D. Ibrahim. In *Salmonella: A Diversified Superbug*, Y. Kumar (Ed.), Chap. 4, pp. 1–26, In Tech, Open Access Company, Croatia, Europe (2012).